Available online at www.sciencedirect.com

SciVerse ScienceDirect

Procedia Technology 3 (2012) 30 – 40

Procedia Technology

The 2012 Iberoamerican Conference on Electronics Engineering and Computer Science

An Exact Solution for the Level-Crossing Rate and the Average Duration of Fades of the Envelope of Sum-of-Cisoids Processes

Matthias Pätzold[a,*], Javier Vázquez Castillo[b], Carlos A. Gutiérrez[c,d], Ramón Parra Michel[b]

[a] *Faculty of Engineering and Science, University of Agder, Grimstad, Norway*
[b] *CINVESTAV-IPN, Unidad Guadalajara, Guadalajara, México*
[c] *Electronics Department, Autonomous University of San Luis Potosí, Av. Salvador Nava Mtz. s/n, San Luis Potosi 78290, México*
[d] *School of Engineering, Panamericana University, Aguascalientes, México*

Abstract

Sum-of-cisoids (SOC) processes provide a physically and numerically appealing framework for the modelling and simulation of a wide class of mobile radio channels. This paper is concerned with the problem of finding a general solution for the level-crossing rate (LCR) and the average duration of fades (ADF) of the envelope of SOC processes. Exact expressions are derived for the LCR and the ADF by taking into account that the inphase component, the quadrature component, and the time derivatives of the inphase and quadrature components of SOC processes are in general mutually correlated. The validity of the theoretical results is confirmed by simulation results. This study reveals new insight into the fading behaviour of SOS-based multipath fading channel models. The results of this study are indispensable for the performance assessment of mobile radio channel simulators employing the SOC principle.

Keywords: Mobile radio channels, fading channel simulators, sum-of-sinusoids, sum-of-cisoids, level-crossing rate, average duration of fades, Rayleigh fading, Rice fading.

1. Introduction

Rice's sum-of-sinusoids (SOS) [1, 2] provides a powerful mathematical tool for the modelling and simulation of mobile radio channels. By computing appropriately the parameters of the SOS model, one can efficiently design a wide class of channel models with given distribution and correlation functions [3, pp. 95 ff.].

In [4], it has been shown that a subclass know as sum-of-cisoids (SOC) process can be derived from two correlated SOS processes. A comparison of SOS and SOC channel models has shown [4, 5] that SOS models are superior to SOC models in case of isotropic scattering. On the other hand, SOC models unleash their full computational power when it comes to the modelling of non-isotropic scattering scenarios, implying

*Corresponding author
Email address: matthias.paetzold@uia.no (Matthias Pätzold)

2212-0173 © 2012 Published by Elsevier Ltd. Open access under CC BY-NC-ND license.
doi:10.1016/j.protcy.2012.03.004

that the Doppler power spectral density has an asymmetric shape. Since this is in general the case in real-world channels, it goes without saying that SOC models are not only the better but the only choice for the modelling and simulation of non-isotropic or measurement-based fading channels. Especially this feature explains why SOC processes have become very attractive candidates in recent years for the modelling of physical channels.

A fundamental analysis of the statistical properties of SOC processes can be found in [4], where expressions have been derived for the correlation functions, power spectral densities, and distribution functions. The interested reader can gain a deeper insight into the statistics of SOC processes from studying [6]. A summary of the most important statistical properties of SOC processes can be found in [3, pp. 126 ff.]. Reference [7] presents a systematic approach to classify all possible types of SOC models. A specific solution to the problem of finding the model parameters of SOC processes under isotropic scattering conditions has been presented in [4]. More general solutions to the parametrization problem under non-isotropic scattering conditions can be found in [5, 8, 9]. Reference [10] presents a generalized method for the design of SOC simulators for the generation of multiple uncorrelated Rayleigh fading channels. The channel capacity of multipath fading channels based on the SOC principle has been analyzed in [11]. Given the rich literature on the modelling and simulation of Rayleigh and Rice fading channels employing the SOC concept, one can now say that the statistical properties of SOC processes are well understood.

One of the last, if not the last, open problem is to find the exact and general expression for the level-crossing rate (LCR) and the average duration of fades (ADF) of the envelope of SOC processes. This problem has first been tackled in [12], where a simple approximate solution as well as a specific exact solution have been derived. The specific exact solution takes into account that the inphase and quadrature components of SOC models are in general correlated. However, to simplify the mathematical analysis, it has been imposed on the model parametrization that the designed SOC process and its time derivative are uncorrelated at the same time. Since this is generally not the case, the approach in [12] leaves space for further improvements. This leads us to the primary motivation of our paper, which can be phrased as follows.

We want to find the general exact expression for the LCR and ADF of the envelope of SOC processes. At the expense of increased mathematical complexity, we show that a solution to this LCR problem indeed exists for any SOC process characterized by constant gains, constant frequencies, and random phases.

The organization of this paper is as follows. Section 2 sets the background by reviewing the main properties of SOC processes. The problem description is presented in Section 3. Section 4 derives exact expressions for the LCR and ADF of the envelope of SOC processes. The correctness of the theory is confirmed in Section 5 by comparing the obtained analytical results with simulation results. Finally, the key findings and conclusions are outlined in Section 6.

2. Review of SOC Processes

Under flat-fading channel conditions, the scattered component of a multipath fading channel can be modelled in the complex equivalent baseband by the following sum of N plane waves (complex sinusoids or cisoids)

$$\hat{\mu}(t) = \sum_{n=1}^{N} c_n e^{\,j(2\pi f_n t + \theta_n)} \tag{1}$$

which defines the SOC process. In the equation above, the parameters c_n, f_n, and θ_n are called the gains, Doppler frequencies, and phases of the nth propagation path, respectively. Depending on the underlying modelling philosophy, each of the parameters can be a constant or a random variable leading to eight classes of channel models with different statistical properties [7]. The focus of this paper is on the statistical properties of SOC processes of Class II [7], which are characterized by constant gains c_n, constant frequencies f_n, and random phases θ_n. It is assumed that the random phases θ_n are independent identically distributed (i.i.d.) random variables uniformly distributed over $(0, 2\pi]$. Under these conditions, the SOC process $\hat{\mu}(t)$ in (1) represents a zero-mean complex stochastic process with variance $\sigma^2_{\hat{\mu}} = \sum_{n=1}^{N} c_n^2$. With reference to

the central limit theorem [13, p. 278], we may conclude that $\hat{\mu}(t)$ tends to a zero-mean complex Gaussian process $\mu(t)$ if the number of cisoids N tends to infinity.

The line-of-sight (LOS) component is assumed to be time invariant and modelled by

$$m = \rho\, e^{j\,\theta_\rho} \tag{2}$$

where ρ and θ_ρ are real-valued constants representing the amplitude and phase, respectively.

By taking the sum of the scattered component $\hat{\mu}(t)$ and the LOS component m, we obtain the nonzero-mean complex random process

$$\hat{\mu}_\rho(t) = \hat{\mu}(t) + m\,. \tag{3}$$

The absolute value of $\hat{\mu}_\rho(t)$, i.e.,

$$\hat{\xi}(t) = |\hat{\mu}_\rho(t)| \tag{4}$$

leads to the SOC simulation model for Rice fading channels. The structure of the resulting SOC simulation model is shown in Fig. 1 in its time-continuous form.

The probability density function (PDF) of the envelope process $\hat{\xi}(t)$ is given by [4]

$$p_{\hat{\xi}}(z) = z(2\pi)^2 \int_0^\infty \left[\prod_{n=1}^{N} J_0(2\pi|c_n|x)\right] J_0(2\pi\, z\, x)\, J_0(2\pi\,\rho\, x)\, x\, dx\,, \quad z \geq 0 \tag{5}$$

where $J_0(\cdot)$ denotes the zeroth-order Bessel function of the first kind. An expression for the cumulative distribution function (CDF) $P_{\hat{\xi}_-}(r)$ of $\hat{\xi}(z)$ can be obtained after substituting (5) into $P_{\hat{\xi}_-}(r) = \int_0^r p_{\hat{\xi}}(z)\, dz$ and solving the integral over z by means of the indefinite integral $\int z J_0(z)\, dz = z J_1(z)$, which can be found in [14, Eq. (5.52-1)]. After performing straightforward algebraic manipulations, the CDF $P_{\hat{\xi}_-}(r)$ can finally be written as

$$P_{\hat{\xi}_-}(r) = 2\pi r \int_0^\infty \left[\prod_{n=1}^{N} J_0(2\pi|c_n|x)\right] J_1(2\pi\, r x)\, J_0(2\pi\,\rho x)\, dx\,, \quad r \geq 0\,. \tag{6}$$

It has been proved in [4] that under the condition $c_n = \sigma_0\sqrt{2/N}$, the PDF $p_{\hat{\xi}}(r)$ in (5) approaches the Rice density

$$p_\xi(z) = \frac{z}{\sigma_0^2} e^{-\frac{z^2+\rho^2}{2\sigma_0^2}} I_0\left(\frac{\tau\rho}{\sigma_0^2}\right), \quad z \geq 0 \tag{7}$$

in the limit $N \to \infty$, where $I_0(\cdot)$ denotes the zeroth-order modified Bessel function of the first kind. In a similar way, it can be shown that the CDF $P_{\hat{\xi}_-}(r)$ in (6) approaches the Rice CDF

$$P_{\xi_-}(r) = 1 - Q\left(\frac{\rho}{\sigma_0}, \frac{r}{\sigma_0}\right), \quad r \geq 0 \tag{8}$$

as $N \to \infty$, where $Q(\cdot,\cdot)$ represents the Marcum Q-function [15].

3. Problem Description

The objective of this paper is to derive a general exact solution for the LCR $N_{\hat{\xi}}(r)$ of the envelope $\hat{\xi}(t)$ of the nonzero-mean SOC process $\hat{\mu}_\rho(t)$ introduced in (3).[1] To solve this problem, we start from Rice's formula

[1] The LCR $N_{\hat{\xi}}(r)$ describes how often the stochastic process $\hat{\xi}(t)$ crosses in average a specified signal level r from down to up (or from up to down) within a time interval of one second.

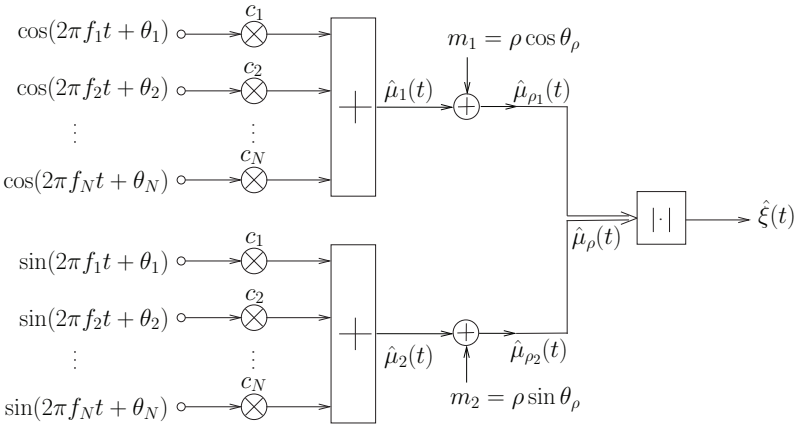

Fig. 1. Structure of an SOC simulation model for Rice fading channels.

for the LCR [1, 2]

$$N_{\hat{\xi}}(r) = \int_0^\infty \dot{z}\, p_{\hat{\xi}\dot{\hat{\xi}}}(r, \dot{z})\, d\dot{z}\,, \quad r \geq 0 \tag{9}$$

which enables us to compute the LCR $N_{\hat{\xi}}(r)$ from the joint PDF $p_{\hat{\xi}\dot{\hat{\xi}}}(z, \dot{z})$ of the envelope $\hat{\xi}(t)$ and its time derivative $\dot{\hat{\xi}}(t)$ at the same time t.[2] It should be mentioned that the expression in (9) is valid for any stationary process. Especially for stationary processes derived from Gaussian random processes, the solution of (9) is computationally straightforward if one starts from the multivariate Gaussian distribution [16, p. 240] and then applying the concept of transformation of random variables [13, p. 244]. The literature is rich with studies of the LCR (ADF) of many different types of mobile radio channels, such as Rayleigh [17, 18], Rice [19], lognormal [20], Suzuki [21, 22, 23], Nakagami [24, 25], and $\alpha - \kappa - \mu$ fading channels [26]. In the present case, however, finding a solution for the LCR $N_{\hat{\xi}}(r)$ is not straightforward. Matters are complicated by the fact that we are dealing here with jointly correlated non-Gaussian processes thwarting the application of the above-mentioned traditional concept.

With reference to (1), it can be shown that the autocorrelation function of $\hat{\mu}(t) = \hat{\mu}_1(t) + j\hat{\mu}_2(t)$, defined by $r_{\hat{\mu}\hat{\mu}}(\tau) = E\{\hat{\mu}^*(t)\,\hat{\mu}(t+\tau)\}$, is given by [4]

$$r_{\hat{\mu}\hat{\mu}}(\tau) = \sum_{n=1}^{N} c_n^2 e^{\,j2\pi f_n \tau}\,. \tag{10}$$

Analogously, the autocorrelation function $r_{\dot{\hat{\mu}}\dot{\hat{\mu}}}(\tau)$ of the time derivative $\dot{\hat{\mu}}(t) = \dot{\hat{\mu}}_1(t) + j\dot{\hat{\mu}}_2(t)$ of $\hat{\mu}(t)$ can be expressed as

$$r_{\dot{\hat{\mu}}\dot{\hat{\mu}}}(\tau) = (2\pi)^2 \sum_{n=1}^{N} (c_n f_n)^2 e^{\,j2\pi f_n \tau} \tag{11}$$

and for the cross-correlation function $r_{\hat{\mu}\dot{\hat{\mu}}}(\tau)$ of $\hat{\mu}(t)$ and $\dot{\hat{\mu}}(t)$, defined by $r_{\hat{\mu}\dot{\hat{\mu}}}(\tau) = E\{\hat{\mu}^*(t)\,\dot{\hat{\mu}}(t+\tau)\}$, we obtain [12]

$$r_{\hat{\mu}\dot{\hat{\mu}}}(\tau) = 2\pi j \sum_{n=1}^{N} c_n^2 f_n e^{\,j2\pi f_n \tau}\,. \tag{12}$$

[2] Throughout this paper, the overdot denotes the time derivative, i.e., $\dot{\hat{\xi}}(t) = d\hat{\xi}(t)/dt$.

The expressions in (10)–(12) clearly demonstrate that the SOC processes $\hat{\mu}_1(t)$, $\hat{\mu}_2(t)$, $\dot{\hat{\mu}}_1(t)$, and $\dot{\hat{\mu}}_2(t)$ are in general mutually correlated, as illustrated in Fig. 2

The problem can now be phrased as follows. We want to find a solution for the LCR $N_{\hat{\xi}}(r)$ under the general condition that the underlying SOC processes $\hat{\mu}_1(t)$, $\hat{\mu}_2(t)$, $\dot{\hat{\mu}}_1(t)$, and $\dot{\hat{\mu}}_2(t)$ are mutually correlated. This problem has first been tackled in [12] under the simplified condition that $\hat{\mu}_i(t)$ and $\dot{\hat{\mu}}_j(t)$ are uncorrelated at the same time t for $i, j = 1, 2$. With reference to Fig. 2, this means that the effect caused by the various intercorrelations has been neglected. On top of this, reference [12] provides also a simple approximate solution, which is very accurate for large values of the number of cisoids N, but the approximation fails if N is small. In this paper, we strive for an exact general solution for the LCR in (9).

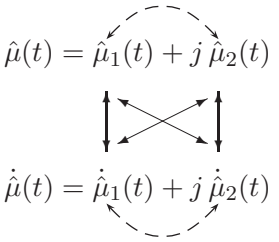

Fig. 2. Illustration of the correlation between the inphase and the quadrature component of SOC processes and their respective time derivatives (intracorrelation: $\leftarrow - \rightarrow$; intercorrelation: $\longleftrightarrow$).

4. Derivation of the LCR and the ADF

4.1. Derivation of the LCR

Let us start by considering a single cisoid $\hat{\mu}_n(t)$ and its time derivative $\dot{\hat{\mu}}_n(t)$ $(n = 1, 2, \ldots, N)$ of the forms

$$\hat{\mu}_n(t) = c_n e^{\,j(2\pi f_n t + \theta_n)} \tag{13a}$$

and

$$\dot{\hat{\mu}}_n(t) = j\,2\pi f_n c_n e^{\,j(2\pi f_n t + \theta_n)} \tag{13b}$$

respectively. In what follows, it is crucial to recall that the gain c_n and frequency f_n are nonzero real-valued constants, and θ_n refers to a random variable with a uniform distribution on $(0, 2\pi]$. For fixed values of t, say $t = t_0$, the nth cisoid $\hat{\mu}_n(t_0) = \hat{\mu}_{1,n}(t_0) + j\hat{\mu}_{2,n}(t_0)$ and its time derivative $\dot{\hat{\mu}}_n(t_0) = \dot{\hat{\mu}}_{1,n}(t_0) + j\dot{\hat{\mu}}_{2,n}(t_0)$ represent random variables, which are statistically dependent, because all components of $\hat{\mu}_n(t_0)$ and $\dot{\hat{\mu}}_n(t_0)$ are controlled by the same random variable θ_n. The distribution of the real part $\hat{\mu}_{1,n}(t_0) = \cos(2\pi f_n t_0 + \theta_n)$ is described by the density [13, p. 135]

$$p_{\hat{\mu}_{1,n}}(x_1) = \begin{cases} \dfrac{1}{\pi c_n \sqrt{1 - (x_1/c_n)^2}}, & |x_1| < c_n \\ 0, & |x_1| \geq c_n\,. \end{cases} \tag{14}$$

Using (14) and extending the concept in [27, Eq. (3.15)] to four random variables, allows us to capture the statistical dependency of the random variables $\hat{\mu}_{1,n}(t_0)$, $\hat{\mu}_{2,n}(t_0)$, $\dot{\hat{\mu}}_{1,n}(t_0)$, and $\dot{\hat{\mu}}_{2,n}(t_0)$ in form of the joint PDF

$$p_{\hat{\mu}_{1,n}\hat{\mu}_{2,n}\dot{\hat{\mu}}_{1,n}\dot{\hat{\mu}}_{2,n}}(x_1, x_2, \dot{x}_1, \dot{x}_2) = p_{\hat{\mu}_{1,n}}(x_1)\,\delta(x_2 - g_1(x_1))\,\delta(\dot{x}_1 - g_2(x_1))\,\delta(\dot{x}_2 - g_3(x_1)) \tag{15}$$

where

$$g_1(x_1) = \begin{cases} c_n \sqrt{1 - (x_1/c_n)^2}, & |x_1| < c_n \\ 0, & |x_1| \geq c_n \end{cases} \tag{16}$$

$$g_2(x_1) = -2\pi f_n \, g_1(x_1) \tag{17}$$

$$g_3(x_1) = 2\pi f_n \, x_1 \, . \tag{18}$$

The joint PDF $p_{\hat{\mu}_{1,n}\hat{\mu}_{2,n}\dot{\hat{\mu}}_{1,n}\dot{\hat{\mu}}_{2,n}}(x_1, x_2, \dot{x}_1, \dot{x}_2)$ in (15) holds the key for the solution of the problem described in the previous section. Continuing with the expression in (15), we can derive the joint PDF $p_{\hat{\xi}\dot{\hat{\xi}}}(z, \dot{z})$ of the envelope $\hat{\xi}(t)$ and its time derivative $\dot{\hat{\xi}}(t)$. After quite intricate mathematical manipulations, we obtain (without proof) the joint PDF $p_{\hat{\xi}\dot{\hat{\xi}}}(z, \dot{z})$ in the following form

$$\begin{aligned} p_{\hat{\xi}\dot{\hat{\xi}}}(z, \dot{z}) \;=\; & 4\pi z \int_0^{\infty}\int_0^{\infty}\int_0^{2\pi} J_0\left(2\pi\rho\, r_1\right)\left[\prod_{n=1}^{N} J_0\Big(2\pi|c_n|\Big\{r_1^2 + (2\pi f_n r_2)^2 \; - 4\pi f_n r_1 r_2 \sin(\theta)\Big\}^{\frac{1}{2}}\Big)\right] \\ & \cdot e^{\,-j2\pi[z\, r_1 \cos(\theta) + \dot{z} r_2]}\, r_1 \, d\theta \, dr_1 \, dr_2 \, . \end{aligned} \tag{19}$$

Notice that $p_{\hat{\xi}\dot{\hat{\xi}}}(z, \dot{z})$ cannot be written as a product of the marginal densities $p_{\hat{\xi}}(z)$ and $p_{\dot{\hat{\xi}}}(\dot{z})$, i.e., $p_{\hat{\xi}\dot{\hat{\xi}}}(z, \dot{z}) \neq p_{\hat{\xi}}(z) \cdot p_{\dot{\hat{\xi}}}(\dot{z})$, which implies that the stochastic processes $\hat{\xi}(t)$ and $\dot{\hat{\xi}}(t)$ are statistically dependent. Now, substituting (19) in (9) results after some few mathematical manipulations in the following final expression for the LCR

$$\begin{aligned} N_{\hat{\xi}}(r) = \; & 4\pi r \int_0^{\dot{z}_{\max}} \dot{z} \int_0^{\infty}\int_0^{\infty}\int_0^{2\pi} J_0(2\pi\rho\, r_1)\left[\prod_{n=1}^{N} J_0\Big(2\pi|c_n|\Big\{r_1^2 + (2\pi f_n r_2)^2 \; - 4\pi f_n r_1 r_2 \sin(\theta)\Big\}^{\frac{1}{2}}\Big)\right] \\ & \cdot e^{\,-j2\pi[r r_1 \cos(\theta) + \dot{z} r_2]}\, r_1 \, d\theta \, dr_1 \, dr_2 \, d\dot{z} \end{aligned} \tag{20}$$

where $\dot{z}_{\max}$ denotes the maximum of $\dot{\hat{\xi}}(t)$, i.e., $\dot{z}_{\max} = \max\{\dot{\hat{\xi}}(t)\} = 2\pi \sum_{n=1}^{N}(f_n c_n)$. The fourfold integral in (20) has to be solved by using numerical integration techniques. The increased mathematical and numerical complexity is associated with the mutually correlated processes $\hat{\mu}_1(t)$, $\hat{\mu}_2(t)$, $\dot{\hat{\mu}}_1(t)$, and $\dot{\hat{\mu}}_2(t)$. This is the price we are willing to pay for the exact and general solution. Without proof, for reasons of brevity, we mention that the LCR $N_{\hat{\xi}}(r)$ in (20) approaches the LCR $N_{\xi}(r)$ of Rice processes in the limit $N \to \infty$, i.e.,

$$\lim_{N\to\infty} N_{\hat{\xi}}(r) = N_{\xi}(r) = \sqrt{\frac{\beta_i}{2\pi}}\, p_{\xi}(r) \tag{21}$$

where $p_{\xi}(r)$ is the Rice density presented in (7), and the quantity β_i is related to the autocorrelation function $r_{\mu_i\mu_i}(\tau)$ of the underlying Gaussian process $\mu_i(t)$ by $\beta_i = -\ddot{r}_{\mu_i\mu_i}(0)$ $(i = 1, 2)$.

4.2. Derivation of the ADF

The mean value of the time intervals over which the process $\hat{\xi}(t)$ remains below a specified threshold level $z = r$ is known as the ADF of $\hat{\xi}(t)$, which is denoted by $T_{\hat{\xi}_-}(r)$. The ADF $T_{\hat{\xi}_-}(r)$ can be obtained using [17, Eq. (1.3–41)]

$$T_{\hat{\xi}_-}(r) = \frac{P_{\hat{\xi}_-}(r)}{N_{\hat{\xi}}(r)} \tag{22}$$

where $P_{\hat{\xi}_-}(r)$ stands for the CDF in (6), and $N_{\hat{\xi}}(r)$ denotes the LCR in (20). Thus, an exact general solution for the ADF $T_{\hat{\xi}_-}(r)$ can easily be obtained by substituting the derived expressions in (6) and (20) in (22). From the statements above, it is obvious that $T_{\hat{\xi}_-}(r)$ tends to the ADF of Rice processes as $N \to \infty$.

5. Numerical Results

The objective of this section is to illustrate the key findings of this paper by numerically evaluating the analytical expressions in (5), (20), and (22). Another objective is to verify the correctness of the analytical results by numerical simulations.

The numerical simulation results have been obtained by evaluating the statistical properties of a set of sample functions generated by using the SOC channel simulator presented in Fig. 1. For the computation of the parameters of the SOC channel simulator, we have invoked the extended method of exact Doppler spread (EMEDS) [3, pp. 222 ff.], which allows us to express the gains c_n and Doppler frequencies f_n in closed form as follows

$$c_n = \sigma_0 \sqrt{\frac{2}{N}} \tag{23}$$

$$f_n = f_{\max} \cos\left[\frac{2\pi}{N}\left(n - \frac{1}{4}\right)\right] \tag{24}$$

for $n = 1, 2, \ldots, N$, where $f_{\max}$ stands for the maximum Doppler frequency. As mentioned in Section 2, the phases θ_n are i.i.d. random variables with a uniform distribution on $(0, 2\pi]$. Let us denote a specific outcome of θ_n by $\theta_n^{(s)}$, then the set of parameters $\{c_n, f_n, \theta_n^{(s)}, \rho, \theta_\rho\}_{n=1}^{N}$ defines completely a sample function[3] $\tilde{\xi}^{(s)}(t)$ of the stochastic process $\hat{\xi}(t)$. In fact, a stochastic process $\hat{\xi}(t)$ is defined by an ensemble of S sample functions $\tilde{\xi}^{(s)}(t)$, i.e., $\hat{\xi}(t) := \{\tilde{\xi}^{(1)}(t), \tilde{\xi}^{(2)}(t), \ldots, \tilde{\xi}^{(S)}(t)\}$. All experimental results presented below have been obtained by evaluating the statistical properties of $S = 100$ sample functions $\tilde{\xi}^{(s)}(t)$ $(s = 1, 2, \ldots, S)$. To investigate the influence of the number of cisoids N on the PDF, LCR, and ADF of $\hat{\xi}(t)$, we studied the cases $N = 10, 20$, and 30. The values of the remaining parameters were set as follows: $f_{\max} = 91$ Hz, $\sigma_0^2 = 1$, $\rho \in \{0, 2\}$, $\theta_\rho = 0$. In the following study, Rayleigh and Rice processes will serve as reference models, which are essential for gaining a better insight into the characteristics of SOC processes.

Figure 3 shows the graphs of the Rayleigh PDF and the Rice PDF, which have been obtained by evaluating (7) for $\rho = 0$ and $\rho = 2$, respectively. Moreover, Fig. 3 illustrates the PDF $p_{\hat{\xi}}(z)$ of the envelope process $\hat{\xi}(t)$. The results have been found by solving numerically the integral in (5) for all considered cases of N and ρ, i.e., $N \in \{10, 20, 30\}$ and $\rho \in \{0, 2\}$. Efficient numerical integration techniques for computing such types of infinite range integrals consisting of an arbitrary product of Bessel functions can be found in [28] and [29]. In addition, Fig. 3 presents the experimental results obtained from the statistical analysis of the sample functions (waveforms) generated by means of the simulation model in Fig. 1. Owing to the perfect match between theoretical and experimental results, we can confirm the validity of the solution for the PDF $p_{\hat{\xi}}(z)$ in (5). Furthermore, we can confirm that the PDF $p_{\hat{\xi}}(z)$ of the envelope of SOC processes is in harmony with the PDF $p_{\xi}(z)$ of Rice and Rayleigh processes if N is not less than 10.

Figure 4 shows a comparative study of the normalized LCR of Rayleigh and Rice processes and the normalized LCR of the envelope of SOC processes. The results for the reference model and the simulation model have been obtained by evaluating (21) and (20), respectively. Figure 4 presents also the experimental results demonstrating the validity of the theoretical results. From these graphs, we can conclude that the LCR of the envelope of SOC processes provides a reasonably good fitting to the LCR of the corresponding reference model if $N = 10$, but noticeable improvements can be achieved by using higher values of N, say $N = 20$. Furthermore, we may conclude that values beyond $N = 20$ do not considerably improve the performance of the SOC model with respect to the LCR.

Figure 5 charts the analogous results obtained for the normalized ADF of the two reference models and the SOC model. Note that the correctness of the theory is once again confirmed by experimental simulations.

Finally, Fig. 6 provides an insight into the relative error $\epsilon_{N_{\hat{\xi}}}(r)$ of the LCR $N_{\hat{\xi}}(r)$, which is defined as

$$\epsilon_{N_{\hat{\xi}}}(r) = \frac{N_{\hat{\xi}}(r) - N_{\xi}(r)}{N_{\xi}(r)} \tag{25}$$

[3] The sample function $\tilde{\xi}^{(s)}(t)$ is also called waveform or deterministic process.

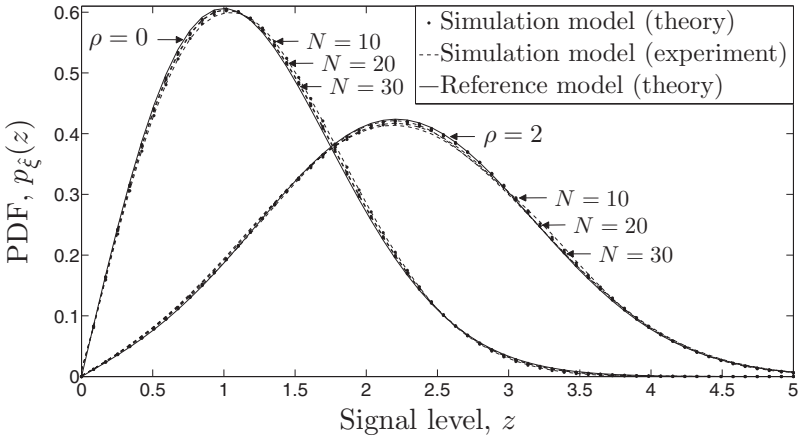

Fig. 3. Comparison of the PDF of Rayleigh ($\rho = 0$) and Rice ($\rho = 2$) processes with the PDF of the envelope of SOC processes $\hat{\xi}(t)$ designed by using the EMEDS with $N \in \{10, 20, 30\}$ ($\sigma_0^2 = 1$, $f_{\max} = 91$ Hz).

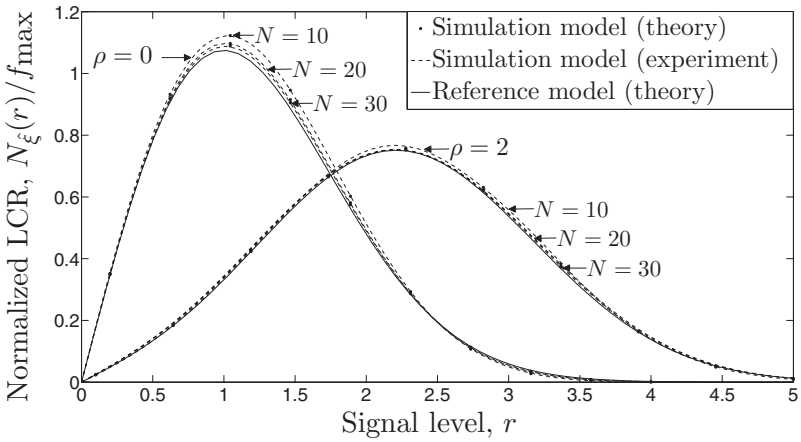

Fig. 4. Comparison of the normalized LCR of Rayleigh ($\rho = 0$) and Rice ($\rho = 2$) processes with the normalized LCR of SOC processes designed by using the EMEDS with $N \in \{10, 20, 30\}$ ($\sigma_0^2 = 1$, $f_{\max} = 91$ Hz).

where $N_{\hat{\xi}}(r)$ and $N_{\xi}(r)$ are denoting the LCR of the SOC model and the reference model as described by (20) and (21), respectively. In Fig. 6, we can clearly realize that there exists obviously a threshold level r_{th} of approximately $r_{\text{th}} = r \approx 2.5$ at which the tangent of the relative error $\epsilon_{N_{\hat{\xi}}}(r)$ passes through zero. Below this threshold level r_{th}, the LCR of the SOC model is larger than that of the reference model, while the inverse statement is true for $r > r_{\text{th}}$. Fortunately, the magnitude of the relative error $\epsilon_{N_{\hat{\xi}}}(r)$ is much smaller for all levels $r < r_{\text{th}}$ than for $r > r_{\text{th}}$. Especially this feature manifests the usefulness of the SOC model as Rayleigh (Rice) fading channel simulator for the performance analysis of mobile radio communication systems. The reason is that the performance of any mobile communication system depends much more on the fading behaviour at low signal levels than it does at high levels. This implies that any useful fading channel simulator must accurately emulate the deep fade statistics, while performance degradations at high signal levels can often be tolerated.

6. Conclusion

This paper has examined the LCR and the ADF of the envelope of SOC processes with constant gains, constant Doppler frequencies, and random phases. In our study, we have taken into account that the inphase

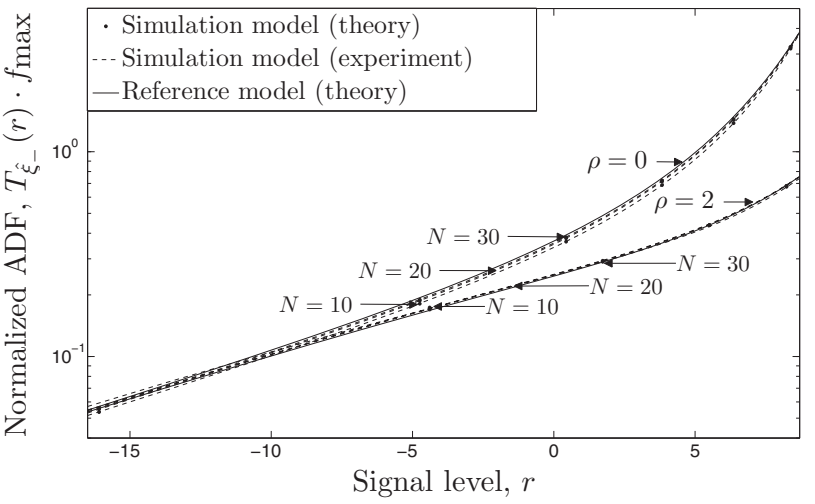

Fig. 5. Comparison of the normalized ADF of Rayleigh ($\rho = 0$) and Rice ($\rho = 2$) processes with the normalized ADF of SOC processes designed by using the EMEDS with $N \in \{10, 20, 30\}$ ($\sigma_0^2 = 1$, $f_{\max} = 91$ Hz).

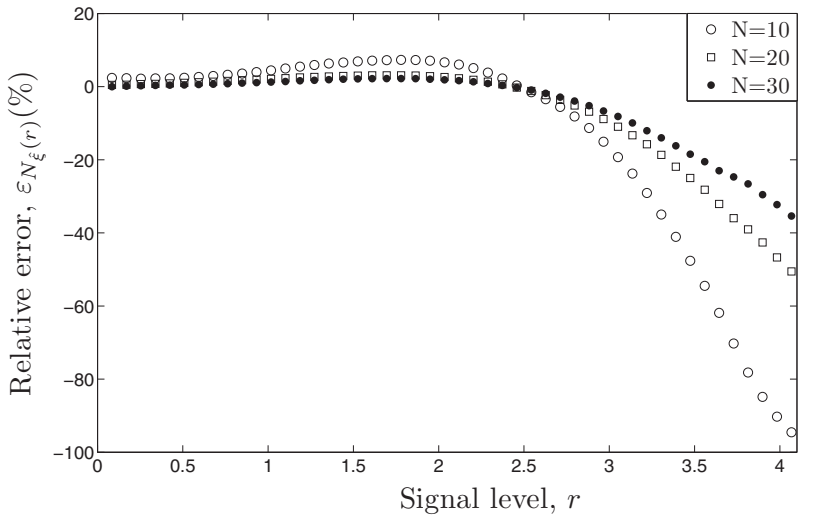

Fig. 6. Relative error $\epsilon_{N_{\dot{\xi}}}(r)$ of the LCR of SOC processes designed by using the EMEDS with $N \in \{10, 20, 30\}$ ($\sigma_0^2 = 1$, $f_{\max} = 91$ Hz, $\rho = 0$).

component, the time derivative of the inphase component, the quadrature component, and the time derivative of the quadrature component of SOC processes are in general mutually correlated. This fact, combined with the cumbersome expression for the distribution of the envelope of SOC processes, makes the theoretical analysis of the LCR (ADF) a difficult task.

In this study, we have found the general and exact solution for the LCR (ADF) of the envelope of SOC processes. Owing to the complexity of the problem, the presented solution requires the use of sophisticated numerical integration techniques. The solution shows that the LCR is not proportional to the PDF of the envelope. This is in contrast to Rayleigh and Rice processes, which serve here as reference models, where the LCR can be expresses simply as a constant multiplied by the corresponding envelope distribution.

From our analysis, we can conclude that the LCR (ADF) of stochastic SOC channel simulators is more sensitive to the model parameters than the envelope distribution. While 10 cisoids can be considered as sufficient for the SOC model to guarantee an excellent fit to the Rayleigh and Rice distributions, we rec-

ommend using approximately twice that number to obtain a fit of the same quality with respect to the LCR (ADF). Furthermore, our analysis has revealed that there exists a threshold signal level around 2.5 at which the relative error of the LCR goes through zero for all values of N. For signal levels below (above) this threshold, we have seen that the LCR of the SOC model is above (below) the LCR of the reference model. We have also demonstrated that even for small values of N, say $N \approx 10$, the relative error of the LCR is only in the order of some few per cent if the signal level is beyond the threshold level, while the relative error increases drastically the larger the signal level exceeds the threshold level.

Given the presented solution of the LCR problem and adding to this the huge amount of research results known from previous studies of SOC processes, we can now safely say that the statistical properties of the SOC process are well understood. This allows us to draw the final conclusion by saying that the theory of SOC processes provides a unified framework for the modelling and simulation of mobile radio channels.

References

[1] S. O. Rice, Mathematical analysis of random noise, Bell Syst. Tech. J. 23 (1944) 282–332.
[2] S. O. Rice, Mathematical analysis of random noise, Bell Syst. Tech. J. 24 (1945) 46–156.
[3] M. Pätzold, Mobile Radio Channels, 2nd Edition, Chichester: John Wiley & Sons, 2011, 583 pages.
[4] M. Pätzold, B. Talha, On the statistical properties of sum-of-cisoids-based mobile radio channel simulators, in: Proc. 10th International Symposium on Wireless Personal Multimedia Communications, WPMC 2007, Jaipur, India, 2007, pp. 394–400.
[5] C. A. Gutiérrez, M. Pätzold, Sum-of-sinusoids-based simulation of flat fading wireless propagation channels under non-isotropic scattering conditions, in: Proc. 50th IEEE Global Communications Conference, IEEE GLOBECOM 2007, Washington DC, USA, 2007, pp. 3842–3846.
[6] C. A. Gutiérrez, Channel simulation models for mobile broadband communication systems, Ph.D. thesis, University of Agder, Norway (2009).
[7] B. O. Hogstad, M. Pätzold, On the stationarity of sum-of-cisoids-based mobile fading channel simulators, in: Proc. IEEE 67th Vehicular Technology Conference, IEEE VTC 2008-Spring, Marina Bay, Singapore, 2008, pp. 400–404.
[8] C. A. Gutiérrez, M. Pätzold, The generalized method of equal areas for the design of sum-of-cisoids simulators for mobile Rayleigh fading channels with arbitrary Doppler spectra, Wireless Communications and Mobile Computing, published online, DOI 10.1002/wcm.1154.
[9] C. A. Gutiérrez, M. Pätzold, The Riemann sum method for the design of sum-of-cisoids simulators for Rayleigh fading channels in non-isotropic scattering environments, in: Proc. IEEE Workshop on Mobile Computing and Network Technologies, WMCNT 2009, St. Petersburg, Russia, 2009.
[10] C. A. Gutiérrez, M. Pätzold, A generalized method for the design of ergodic sum-of-cisoids simulators for multiple uncorrelated Rayleigh fading channels, in: Proc. 4th International Conference on Signal Processing and Communication Systems, ICSPCS 2010, Gold Coast, Australia, 2010, DOI 10.1109/ICSPCS.2010.5709688.
[11] G. Rafiq, M. Pätzold, Statistical properties of the capacity of multipath fading channels, in: Proc. IEEE International Symposium on Personal, Indoor and Mobile Radio Communications, PIMRC 2009, Tokyo, Japan, 2009, pp. 1103–1107.
[12] M. Pätzold, C. A. Gutiérrez, Level-crossing rate and average duration of fades of the envelope of a sum-of-cisoids, in: Proc. IEEE 67th Vehicular Technology Conference, IEEE VTC 2008-Spring, Marina Bay, Singapore, 2008, pp. 488–494.
[13] A. Papoulis, S. U. Pillai, Probability, Random Variables and Stochastic Processes, 4th Edition, New York: McGraw-Hill, 2002.
[14] I. S. Gradshteyn, I. M. Ryzhik, Table of Integrals, Series, and Products, 6th Edition, Academic Press, 2000.
[15] J. I. Marcum, A statistical theory of target detection by pulsed radar, IEEE Trans. Inform. Theory 6 (2) (1960) 59–267.
[16] A. Leon-Garcia, Probability and Random Processes for Electrical Engineering, 2nd Edition, Addison Wesley Publishing Company, 1994.
[17] W. C. Jakes (Ed.), Microwave Mobile Communications, Piscataway, NJ: IEEE Press, 1994.
[18] G. D. Durgin, T. S. Rappaport, Level-crossing rates and average fade duration for wireless Ricean fading channels with spatially complicated multipath, in: Proc. IEEE Global Communications Conference, IEEE GLOBECOM 1999, Rio de Janeiro, Brazil, 1999, pp. 427–431.
[19] S. O. Rice, Statistical properties of a sine wave plus random noise, Bell Syst. Tech. J. 27 (1948) 109–157.
[20] M. Pätzold, K. Yang, An exact solution for the level-crossing rate of shadow fading processes modelled by using the sum-of-sinusoids principle, in: Proc. 9th International Symposium on Wireless Personal Multimedia Communications, WPMC 2006, San Diego, USA, 2006, pp. 188–193.
[21] A. Krantzik, D. Wolf, Distribution of the fading-intervals of modified Suzuki processes, in: L. Torres, E. Masgrau, M. A. Lagunas (Eds.), Signal Processing V: Theories and Applications, Amsterdam, The Netherlands: Elsevier Science Publishers, B.V, 1990, pp. 361–364.
[22] A. Krantzik, D. Wolf, Statistische Eigenschaften von Fadingprozessen zur Beschreibung eines Landmobilfunkkanals, FREQUENZ 44 (6) (1990) 174–182.
[23] M. Pätzold, U. Killat, F. Laue, An extended Suzuki model for land mobile satellite channels and its statistical properties, IEEE Trans. Veh. Technol. 47 (2) (1998) 617–630.
[24] N. Youssef, T. Munakata, M. Takeda, Fade statistics in Nakagami fading environments, in: Proc. IEEE 4th Int. Symp. on Spread Spectrum Techniques & Applications, ISSSTA'96, Mayence, Germany, 1996, pp. 1244–1247.

[25] M. D. Yacoub, J. E. V. Bautista, L. G. de Rezende Guedes, On higher order statistics of the Nakagami-*m* distribution, IEEE Trans. Veh. Technol. 48 (3) (1999) 790–794.
[26] A. K. Papazafeiropoulos, S. A. Kotsopoulos, Second-order statistics for the envelope of α - κ - μ fading channels, IEEE Communications Letters 14 (4) (2010) 291–293.
[27] S. Primak, V. Kontorovich, V. Lyandres, Stochastic Methods and their Applications to Communications – Stochastic Differential Equations Approach, Chichester: John Wiley & Sons, 2004.
[28] J. V. Deun, R. Cools, Algorithm 858: Computing infinite range integrals of an arbitrary product of Bessel functions, ACM Transactions on Mathematical Software 32 (4) (2006) 580–596.
[29] J. V. Deun, R. Cools, Integrating products of Bessel functions with an additional exponential or rational factor, Computer Physics Communications 178 (8) (2008) 578–590.